

Turbulent velocity distributions and implied trajectory models

John D. Wilson

Received: 1 September 2006 / Accepted: 22 March 2007 / Published online: 3 July 2007
© Springer Science+Business Media, B.V. 2007

Abstract Well-mixed, first-order Lagrangian stochastic (LS) particle trajectory models are derived from several idealized (“toy”) turbulent velocity distributions, and their performance is compared against the observations of Project Prairie Grass, i.e., the case of a continuous point source of tracer near the ground, in the horizontally homogeneous and neutrally stratified surface layer. Although in a context of limited information a Gaussian distribution is the preferred choice, and although the Gaussian corresponds to the simplest of this set of LS models (namely, the Langevin equation), models stemming from other velocity distributions give similar, albeit distinguishable, predictions.

Keywords Dispersion models · Lagrangian stochastic models · Turbulent dispersion · Velocity distribution functions · Well-mixed condition

1 Introduction

This note stems from the author’s initial surprise upon reading that the function $f(x) = \alpha/(1 + \beta x^2)$ cannot for any choice of α, β represent a probability density function (PDF), if the random variable x has the range $-\infty \leq x \leq \infty$ (integral for the variance diverges). This (in hindsight, obvious) fact prompted an accentuated curiosity about the forms of PDFs that *are* acceptable, and in particular the particle trajectory models they imply.

Assume a stationary turbulent flow in which the velocity statistics are uniform, not only on horizontal planes, but (also) along the vertical axis (our focus will be the horizontally uniform and neutrally stratified atmospheric surface layer, or wall shear layer: the ‘hhNSL’). The one-dimensional, first-order Lagrangian stochastic (LS) model for the vertical component

J. D. Wilson (✉)

Department of Earth & Atmospheric Sciences, University of Alberta, Edmonton, Canada
e-mail: jaydee.uu@alberta.ca

($W = dZ/dt$) of the motion¹ of a marked fluid element is

$$dW = a(Z, W) dt + \sqrt{C_0 \epsilon} d\xi, \quad (1)$$

$$dZ = W dt \quad (2)$$

where $\epsilon(z)$ is the rate of dissipation of turbulent kinetic energy (TKE, k), C_0 is the coefficient appearing in Kolmogorov's theoretical expression for the expected value of $\langle dW^2 \rangle$ ($= C_0 \epsilon dt$) for small dt , and $d\xi$ is a Gaussian random variate with vanishing mean and variance dt . The well-mixed condition (Thomson 1987; Eq. 9a,b) requires that

$$a = \frac{1}{2} C_0 \epsilon \frac{\partial \ln g_a(w)}{\partial w} + \frac{\phi(w)}{g_a(w)}, \quad (3)$$

$$\frac{\partial \phi}{\partial w} = -w \frac{\partial g_a}{\partial z} \quad (4)$$

and with our restriction that the PDF $g_a(w)$ of the Eulerian vertical velocity has constant moments, it follows that

$$a = \frac{1}{2} C_0 \epsilon \frac{\partial \ln g_a(w)}{\partial w}. \quad (5)$$

The intent of this note is to examine an interesting if arcane aspect of LS models, namely, the extent to which we have freedom to build them from whatever velocity distribution we might consider auspicious.

2 The 'true' velocity PDF in turbulent flow

Sufficiently far from the boundaries of a turbulent shear layer, the observed Eulerian PDF is closely Gaussian. Batchelor (1953, Ch. 8) cites some of the early evidence of this, along with a heuristic explanation by way of the Central Limit Theorem (a much stronger explanation, due to Pope, is given below; and see also Mouri et al. 2002). In short, in the words of Falkovich and Lebedev (1997) "early experimental data on skewness and flatness of the velocity field prompted one to believe that the single-point velocity PDF in developed turbulence is generally close to Gaussian", and any observed slight non-Gaussianity could be attributed (e.g. Maxey 1987) to instrument error or inhomogeneity or non-stationarity. The earliest observations focused on laboratory grid turbulence, but there are now observations in the wall shear layer, e.g. Österlund and Johansson (1999, their Fig. 22) give PDFs of streamwise velocity in a zero pressure gradient wall shear layer, showing that over much of the region $(0.1-0.8)\delta$ the PDF is close to Gaussian (δ is the boundary-layer depth). Observations in the stratified atmospheric surface layer (e.g. Chu et al. 1996) also support the choice of a Gaussian.

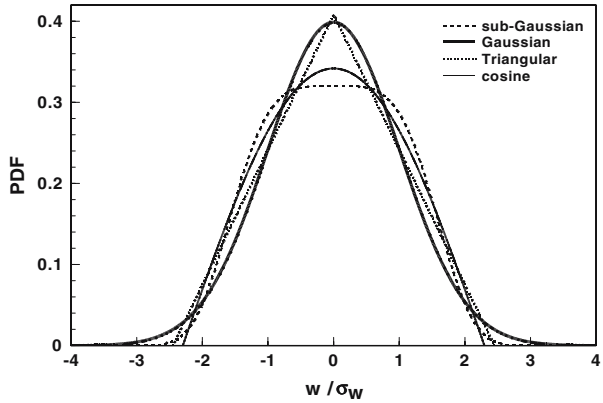
From a theoretical stance, none of this is surprising. Pope (2000) gives the exact evolution equation for the velocity PDF and shows that, upon adopting simple closures for unknown terms, it contains a diffusion term, i.e.

$$\frac{\partial g}{\partial t} = \frac{\partial}{\partial v_i} (g a_i v_i) + \frac{1}{2} C_0 \epsilon \frac{\partial^2 g}{\partial v_i \partial v_i} \quad (6)$$

where $a_i v_i g$ is the flux of g along the v_i -axis. Consequently no matter what the initial form of the velocity PDF, it is asymptotically Gaussian. Pope states that "For the general case, the

¹ Particle position and velocity will be denoted by upper case Z, W while z is the vertical coordinate and w the Eulerian velocity fluctuation.

Fig. 1 Comparison of several symmetric and standardized probability density functions (PDFs) defined in the text (w/σ_w is the independent variable)



qualitative behaviour of the generalized Langevin model (for the behaviour of the PDF) is the same as (this). The drift term deforms the PDF without qualitatively affecting its shape; while the diffusion term makes it tend towards an isotropic joint normal. For homogeneous turbulence... the solution tends to a joint normal from any initial condition. This is the correct physical behaviour...”

There are other reasons for the commonness of the choice of a Gaussian PDF, including the fact that commonly it represents the “maximum missing information” PDF, i.e. for a single random variate whose mean and variance (alone) are given, the Gaussian is maximally “agnostic” with respect to unknown quantities (e.g. Du et al. 1994a, b). Furthermore we tend to consider that in a quite general sense the Gaussian is “normal”, which presumably is why we also label it the “Normal” distribution. And finally, one of the attributes we recognize in turbulence is disorganization (whereas organization or coherency of turbulence is the attribute determining the degree of non-Gaussianity of the velocity PDF), which implies we should expect to find a continuum of eddy sizes and topologies and intensities—in view of which it would be surprising to observe ‘gaps’ in the PDF (low probability of certain velocities), or discontinuities in its slope. Thus the ‘disorganization’ of a turbulent flow suggests we should expect a smooth velocity PDF (assuming, of course, that sampling error is eliminated), i.e. continuous g_a and $\partial g_a / \partial u_i$.

3 Some ‘simple’ symmetric velocity PDF’s and implied LS models

Figure 1 compares the standardized Gaussian PDF

$$g_a(w) = \frac{1}{\sqrt{2\pi} \sigma_w} \exp\left(-\frac{w^2}{2 \sigma_w^2}\right) \tag{7}$$

with three other (arbitrarily chosen) functions, all sharing the necessary normalization property (unit area) and all, like the Gaussian,² symmetric about the coincident and vanishing mean, median and mode:

² Recall that all moments of the Gaussian PDF can be expressed in terms of the mean and variance; the kurtosis (flatness) $F = 3$; curvature vanishes at $w = \pm\sigma_w$ and is concave at $|w| > \sigma_w$. A super- (or hyper-) Gaussian PDF has kurtosis (flatness) factor $F > 3$, while a sub- (or hypo-) Gaussian has $F < 3$.

- The triangular PDF

$$g_a(w) = \begin{cases} \frac{1}{\alpha \sigma_w} \left(1 - \frac{|w|}{\alpha \sigma_w}\right) & |w| \leq \alpha \sigma_w \\ 0 & |w| > \alpha \sigma_w \end{cases} \tag{8}$$

which correctly reproduces the variance if the span parameter $\alpha = \sqrt{6}$.

- The truncated cosine PDF

$$g_a(w) = \begin{cases} \frac{\pi}{4 \alpha \sigma_w} \cos\left(\frac{\pi}{2} \frac{w}{\alpha \sigma_w}\right) & |w| \leq \alpha \sigma_w \\ 0 & |w| > \alpha \sigma_w \end{cases} \tag{9}$$

which is normalized if $\alpha = 1/\sqrt{1 - 8/\pi^2}$.

- The sub-Gaussian

$$g_a(w) = \frac{1}{\gamma^* \sigma_w} \exp\left(-\frac{w^4}{4 \gamma \sigma_w^4}\right) \tag{10}$$

for which normalization and calibration demand

$$\gamma = 2^{-5/2} \left[\frac{\Gamma(1/4)}{\Gamma(3/2)}\right]^2 = 2.18858, \tag{11}$$

$$\gamma^* = 2 (4\gamma)^{-1/4} / \Gamma(1/4) = 3.11822 \tag{12}$$

and for which the flatness $F \approx 2.2$.

The point of this comparison is that it is easy to arrange a curve whose area is distributed (roughly) in the same manner as the Gaussian. We have seen that the Gaussian has the best pedigree from almost every perspective, i.e. the others are poor candidates physically. But suppose they were attractive candidates mathematically. Would a great penalty be paid if one invoked a PDF that is wrong as regards the wanted symmetries and continuity, and which fails to correctly model higher moments? In this context note that [Taylor \(1921\)](#) showed that the standard deviation of the particle displacement PDF (i.e. the mean concentration distribution) in stationary, homogeneous turbulence is sensitive (explicitly and directly) to the standard deviation of (Lagrangian) velocity, but (except in the near field of the source) indifferent to the details of velocity autocorrelation. Thus the earliest Lagrangian theory, and still more so the overwhelmingly predominant eddy diffusion approach, amounted to a framework for thinking within which there was no explicit role for the turbulent velocity PDF (other than its variance); indeed as noted at the outset, the criteria provided by [Thomson \(1987\)](#) have greatly clarified the relationship between (modelled) dispersion and the underlying velocity PDF.

Table 1 gives the conditional mean acceleration a for each of the PDFs of Fig. 1. What is striking is that, although the Gaussian PDF does not stand out as *mathematically* the simplest of those considered, it gives by far the simplest well-mixed LS model, namely the classical Langevin equation. Interestingly the sub-Gaussian PDF leads to a Langevin-like model but with the stabilizing memory term proportional to $-W^3$ in lieu of $-W$.

4 Performance of LS models implied by these PDFs

The neutrally stratified, horizontally homogeneous surface layer ('hhNSL') is the simplest environmental regime of inhomogeneous turbulence, and it seemed interesting to compare the performance of these well-mixed LS models in simulating tracer dispersion for that

Table 1 Several possible symmetric velocity PDFs $g(w)$ and the implied (antisymmetric) conditional mean acceleration $a(w) \equiv \frac{1}{2} C_0 \epsilon \partial \ln g(w)/\partial w$ for a one-dimensional, well-mixed LS model of tracer paths in the neutral wall shear layer

| $g(w) \propto$ | $(w /\sigma_w)_{\max}$ | Kurtosis (F) | $\partial \ln g(w)/\partial w$ |
|--|-------------------------|------------------|---|
| $\exp\left(-\frac{w^2}{2\sigma_w^2}\right)$ | ∞ | 3 | $-w/\sigma_w^2$ |
| $\exp\left(-\frac{w^4}{4\gamma\sigma_w^4}\right)$ | ∞ | 2.19 | $-\gamma w^3/\sigma_w^4$ |
| $1 - w /(\alpha \sigma_w)$ | α | 2.40 | $-w/\left[\alpha \sigma_w w - w^2\right]$ |
| $\cos\left(\frac{\pi}{2} \frac{w}{\alpha \sigma_w}\right)$ | α | 2.19 | $-\pi(2\alpha\sigma_w)^{-1} \tan\left[\pi w(2\alpha\sigma_w)^{-1}\right]$ |

case (in the interest of simplicity, the streamwise velocity fluctuations was not modelled, past experience having shown its influence is small for the problem examined here). All simulations to be shown were performed with $b = \sigma_w/u_* = 1.25$, $C_0 = 3.125$, which ensures that the eddy diffusivity implied in the ‘diffusion limit’ (e.g. Sawford and Guest 1988) of the Ito stochastic differential equation (1) is

$$K = \frac{k_v}{S_c} u_* z \tag{13}$$

with turbulent Schmidt number $S_c = 0.64$ (here $k_v = 0.4$ is the von Karman constant and u_* the friction velocity). Although many flux-gradient experiments (e.g. Dyer and Bradley 1982) have indicated equality of the eddy diffusivity and eddy viscosity ($\nu_T = k_v u_* z$) in the hhNSL, tracer experiments have indicated otherwise, e.g. for Project Prairie Grass $S_c \approx 0.6-0.7$ (Wilson et al. 1981; Sawford 2001). The particular choice made here is exactly consistent with earlier simulations by Wilson (1982b), but indistinguishable results were obtained with $b = \sigma_w/u_* = 1.3$, $C_0 = 3.599$ (which imply $S_c = 0.63$). For the following simulations the timestep was specified as

$$dt = \mu \frac{2\sigma_w^2}{C_0\epsilon} \tag{14}$$

where

$$\epsilon = \frac{u_*^3}{k_v z} \tag{15}$$

and in all simulations shown $\mu = 0.02$, the choice $\mu = 0.05$ having proved insufficiently small.

Using the simple Euler method to integrate Eq. 1 an instability was experienced for the triangular and truncated cosine PDFs. This is understandable because in both cases the conditional mean acceleration $a(w)$ provides an *unbounded* restoring force as $|w| \rightarrow \alpha\sigma_w$, e.g. (for the triangular PDF)

$$a = \frac{1}{2} C_0 \epsilon \left(\frac{-w}{\alpha \sigma_w |w| - w^2} \right). \tag{16}$$

The instability was (crudely) overcome by imposing a stronger limit, viz. $|w/\sigma_w| \leq (\alpha - 0.1)$.

4.1 Vertical concentration profile for Project Prairie Grass

In the Project Prairie Grass (PPG) experiments (Barad 1958; Haugen 1959) an array of detectors determined the mean concentration field due to a continuous source (of known strength Q , kg s^{-1}) of sulphur dioxide near ground (height of the source $h_s = 0.46\text{ m}$), and in this section we focus on the vertical profile of crosswind-integrated concentration $\chi = \chi(x, z)$, observed $x = 100\text{ m}$ downstream from the source. The PPG observations of Fig. 2 represent an average over nine near-neutral runs, the averaging (across runs, at each height) being performed on the normalized variable $u_* \chi / Q$ that is invariant relative to mean wind speed (scaling with the friction velocity u_*) and source strength.

Concentration profiles for each of the LS models were computed from ensembles of trajectories in the usual manner (residence time in finite-volume detectors, whose depth was set at 0.2 m). The roughness length was held constant ($z_0 = 0.006\text{ m}$) across all runs, and trajectories were reflected at $Z = z_0$. Figure 2 shows that all four PDFs result in LS models that are in tolerably good agreement with the observations. It is interesting that although the truncated cosine and the sub-Gaussian PDFs have nearly equal values of kurtosis ($F = 2.2$) in addition (of course) to reproducing the correct mean and variance, they result in distinguishable concentration profiles. The profile produced by the LS model based on the sub-Gaussian PDF differs most from the other curves, and is probably the least satisfactory. As Fig. 1 shows, this is the PDF differing most greatly from the Gaussian in the frequently sampled region in the neighbourhood of the mean, and one may speculate that (in combination with the imposed surface reflection) the dearth of small $|w|$ associated with the sub-Gaussian PDF may explain the accelerated rate of vertical dispersion.

4.2 Horizontal transect of ground-level concentration

With the source placed at ground in the hhNSL, surface concentration as a function of downwind distance was deduced from mean particle residence time in bins that, at fetch x/z_0 , spanned $1 \leq z/z_0 \leq 0.005x/z_0$. Cross-wind integrated surface concentration $\chi_0(x)$ varies roughly as $\chi_0 \propto x^{-1}$, and so Fig. 3 presents the transect of the (asymptotically constant) re-normalized concentration $\Phi = \chi_0(x) u_* x (k_v Q)^{-1}$, where k_v is inserted merely for consistency with earlier convention. The solid symbols stem from a tabulation by Wilson (1982b, Table 1, “Line, $\Omega = 0$ ”), from calculations using the unique well-mixed LS model for (one-dimensional) Gaussian inhomogeneous turbulence. They differ from the present calculation based on the Gaussian PDF in that the W82 simulation was performed in the z_* ($\propto \ln z$) coordinate system (e.g. Wilson et al. 1981; Wilson and Yee 2007), such that (computationally) the turbulence is homogeneous, obviating Δt bias error and legitimizing surface reflection (Wilson and Flesch 1993). The other reference is the analytical solution of Wilson (1982a; also summarized in the appendix of Wilson and Yee 2007), an eddy-diffusion solution that (not accidentally, because the Schmidt number had been propitiously chosen) is consistent with Project Prairie Grass and the Lagrangian solutions.

The performance of the four LS models is more easily distinguishable in this ground-level transect than in the profile at $x = 100\text{ m}$, with a spread $\delta\Phi \approx 0.5$ (as also can be deduced by rescaling the spread at ground on Fig. 2). Once again, outcomes do not stratify in relation to the kurtosis of the PDF. Perhaps this relates to the stabilizing intervention alluded to above, which (in the case of the triangular and truncated cosine PDFs) must to some extent have distorted the actual PDF.

Fig. 2 First-order Lagrangian stochastic simulations of the vertical profile of crosswind-integrated concentration at distance $x = 100\text{ m}$ ($x/z_0 = 1.67 \times 10^4$) downstream from a continuous, near-ground point source, based on the different approximations for the Eulerian velocity PDF. Simulations are compared with the average of nine near-neutral Project Prairie Grass runs (Nos. 21,33,42,57,37,24,38,45,20. The error bar gives sample standard deviation)

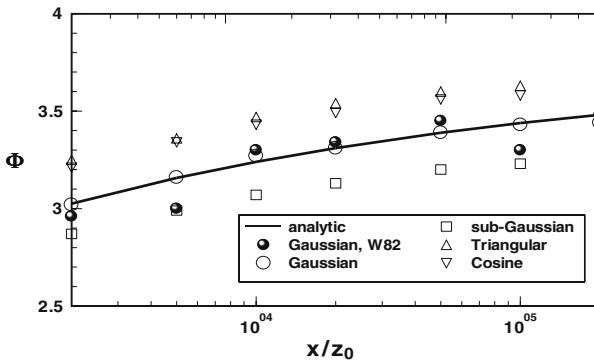
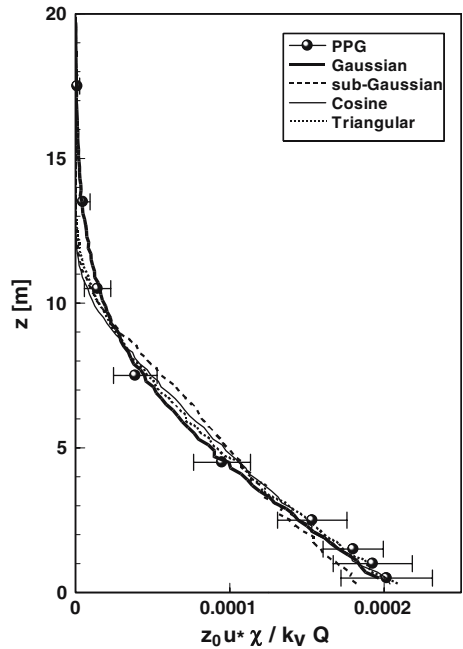


Fig. 3 First-order Lagrangian stochastic simulations of the horizontal transect of (normalized) crosswind-integrated, ground-level concentration $\Phi = \chi_0 u_* x (k_v Q)^{-1}$ for a continuous ground-level source in the hhNSL. Simulations (3.8×10^6 paths) based on four different approximations for the Eulerian velocity PDF are compared with earlier ‘reference’ calculations (heavy line and heavy symbols; see text for explanation) that are consistent with Project Prairie Grass

5 Conclusion

First-order LS models³ have been derived and tested for each of four simple Eulerian velocity PDFs. The point of the exercise was not to seek some ‘better PDF’, but merely to indulge

³ The diffusion limit of the Langevin model is the zeroth-order ‘Random Displacement Model’, $dZ = (\partial K / \partial z) dt + \sqrt{2K} d\xi$, which is equivalent to an eddy-diffusion treatment and known (Wilson and Yee 2007) to provide a simulation that differs only modestly from the reference data (since at the distances considered, one is in the far field of the source). The present findings (Fig. 3) suggest that diffusion the limit of the other first-order LS models is distinct from that of the Langevin model.

a curiosity as to what constitutes ‘simplicity’ and how differently these LS models might perform. It turns out that the alternative models provide concentration transects that (for the case examined) are quite distinct. Occam’s razor, custom, the principles of statistical inference, and physical insight all suggest the adoption of a Gaussian velocity PDF in a system whose moments higher than the second are unknown, for the implied one-dimensional LS model is *simplest*, indeed it is none other than the classical Langevin equation. Furthermore

$$dW = -\frac{W}{T_L} dt + \sqrt{C_0\epsilon} d\xi \quad (17)$$

or (equivalently) the algorithm

$$W^{n+1} = \left(1 - \frac{dt}{T_L}\right) W^n + \sqrt{C_0\epsilon} d\xi \quad (18)$$

amounts to the simplest digital procedure to produce a sequence $W^0, W^1, W^2, \dots, W^n$ having the desired variance σ_w^2 and autocorrelation $T_L = 2\sigma_w^2/(C_0\epsilon)$ from a white noise signal.

Probably the main surprise and most important lesson emerging from the work was the necessity that the timestep $\mu = dt/T_L$ be so small in order to produce the consistency (manifest in Fig. 3) of these simulations with earlier results that are known to be consistent with observations. Such a stringent restriction ($\mu = 0.02$) was not needed for the earlier implementation of the Gaussian-based, i.e. Langevin model, in $\ln(z)$ space, and the need here for such a small value only emerged in the context of a focus on *surface* concentration, where the spread across the different models is most strongly evident. This finding is also pertinent in the context of a study (Wilson and Yee 2007) of the simpler Random Displacement Model (RDM), wherein it is shown that that model (too) demands rather a small timestep for the hhNSL dispersion problem studied.

The preceding discussion may have over-emphasized the ubiquity of the Gaussian velocity PDF. An important counter-example, i.e. a common system of non-Gaussian boundary-layer turbulence, is the convective boundary layer (CBL), which owing to the drifting thermals and the generally sinking environment around them might appropriately be regarded as horizontally inhomogeneous, but which for convenience we conceptualize as being horizontally uniform, with a skew PDF of vertical velocity. In the bulk of the CBL a skew PDF provides a better model than the Gaussian (e.g. Luhar and Britter 1989; Weil 1990; Du et al. 1994b). Similarly it is well known that within a canopy layer (e.g. tall forest or crop) the PDFs of the streamwise and vertical components are respectively positively and negatively skewed, owing to the dominance of this flow by intermittent gusts. However in this case, notwithstanding that velocity statistics are skew near the ground, properly incorporating the consequences of inhomogeneity in that region seems to be more significant than accounting for non-Gaussianity (Flesch and Wilson 1992; Cassiani et al. 2005).

Acknowledgements This work has been supported by research grants from the Natural Sciences and Engineering Research Council of Canada (NSERC) and the Canadian Foundation for Climate and Atmospheric Sciences (CFCAS).

References

- Barad ML (1958) Project Prairie Grass, a field program in diffusion vol 2. Technical report geophysical research papers No. 59, TR-58-235(II). Air Force Cambridge Research Center
- Batchelor GK (1953) The theory of homogeneous turbulence. Cambridge University Press, UK, 197pp

- Cassiani M, Radicchi A, Giostra U (2005) Probability density function modelling of concentration in and above a canopy layer. *Agric Forest Meteorol* 133:153–165
- Chu CR, Parlange MB, Katul CG, Albertson JD (1996) Probability density functions of turbulent velocity and temperature in the atmospheric surface layer. *Water Resour Res* 32:1681–1688
- Du S, Wilson JD, Yee E (1994a) On the moments approximation method for constructing a Lagrangian stochastic model. *Boundary-Layer Meteorol* 70:273–292
- Du S, Wilson JD, Yee E (1994b) Probability density functions for velocity in the convective boundary layer, and implied trajectory models. *Atmos Environ* 28:1211–1217
- Dyer AJ, Bradley EF (1982) An alternative analysis of flux-gradient relationships at the 1976 ITCE. *Boundary-Layer Meteorol* 22:3–19
- Falkovich G, Lebedev V (1997) Single-point velocity distribution in turbulence. arXiv:chao-dyn, 9708002
- Flesch TK, Wilson JD (1992) A two-dimensional trajectory simulation model for non-gaussian, inhomogeneous turbulence within plant canopies. *Boundary-Layer Meteorol* 61:349–374
- Haugen DA (1959) Project Prairie Grass, a field program in diffusion, vol. 3. Technical report geophysical research papers No. 59, TR-58-235(III). Air Force Cambridge Research Center
- Luhar AK, Britter RE (1989) A random walk model for dispersion in inhomogeneous turbulence in a convective boundary layer. *Atmos Environ* 23: 1911–1924
- Maxey MR (1987) The velocity skewness measured in grid turbulence. *Phys Fluids* 30:935–938. doi:10.1063/1.866279
- Mouri H, Takaoka M, Hori A, Kawashima Y (2002) Probability density function of turbulent velocity fluctuations. *Phys Rev E* 65:056304-1–056304-7. DOI: 10.1103/PhysRevE.65.056304
- Österlund JM, Johansson AV (1999) Turbulence statistics of zero pressure gradient turbulent boundary layers. (pp 59–92 in Österlund JM, “Experimental studies of zero pressure gradient boundary layer flow”, PhD thesis, Dept of Mechanics, Royal Inst Technology, Stockholm, 1999)
- Pope SB (2000) *Turbulent flows*. Cambridge University Press, UK, 806pp
- Sawford BL (2001) Project Prairie Grass—a classic atmospheric dispersion experiment revisited. 14th Australian fluid mech conference
- Sawford BL, Guest FM (1988) Uniqueness and universality of Lagrangian stochastic models of turbulent dispersion. Preprints of 8th Symp. Of the AMS on Turbulence and Diusion, San Diego, CA. American Meteorological Society, for American Meteorological Society pp 96–99
- Taylor GI (1921) Diffusion by continuous movements. *Proc London Math Soc Ser 2*(A20):196–211
- Thomson DJ (1987) Criteria for the selection of stochastic models of particle trajectories in turbulent flows. *J Fluid Mech* 180:529–556
- Weil JC (1990) A diagnosis of the asymmetry in top-down and bottom-up diusion using a Lagrangian stochastic model. *J Atmos Sci* 47:501–515
- Wilson JD (1982a) An approximate analytical solution to the diffusion equation for short-range dispersion from a continuous ground-level source. *Boundary-Layer Meteorol* 23:85–103
- Wilson JD (1982b) Turbulent dispersion in the atmospheric surface-layer. *Boundary-Layer Meteorol* 22:399–420
- Wilson JD, Flesch TK (1993) Flow boundaries in random flight dispersion models: enforcing the well-mixed condition. *J Appl Meteorol* 32:1695–1707
- Wilson JD, Yee E (2007) A critical examination of the random displacement model of turbulent dispersion. *Boundary-Layer Meteorol* (in press) doi: 10.1007/s10546-007-9201-x
- Wilson JD, Thurtell GW, Kidd GE (1981) Numerical simulation of particle trajectories in inhomogeneous turbulence. III. Comparison of predictions with experimental data for the atmospheric surface-layer. *Boundary-Layer Meteorol* 21:443–463